Fast Separation of Specular, Diffuse, and Global Components via Polarized Pattern Projection

Yuto Nisaka[1], Ryo Matsuoka[2], Toshiyuki Amano[3], and Takahiro Okabe[1][0000−0002−2183−7112]

[1] Kyushu Institute of Technology
okabe@ai.kyutech.ac.jp
[2] The University of Kitakyushu
[3] Wakayama University

Abstract. In this paper, we propose a method for fast separation of specular, diffuse, and global components of a dynamic scene by using a projector-camera system. Both the direct-global separation using spatially high-frequency patterns and the specular-diffuse separation based on polarization have been studied, but a straightforward combination of those methods has limited temporal resolution. Accordingly, our proposed method rapidly changes not only the spatial patterns but also the polarization states of illumination by using a self-build polarization projector, and captures their effects on a scene by using a high-speed camera. Our method is easy-to-implement, because it does not require projector-camera temporal synchronization and it automatically calibrates the correspondence between the projection pattern and camera pixel. In addition, our method is robust due to the optimized and quickly-shifted projection pattern and the weights for incorporating spatial correlation. We implemented the prototype setup and achieved fast separation with 60 fps.

Keywords: direct-global separation · specular-diffuse separation · projector-camera system · polarization

1 Introduction

When a scene is illuminated by a light source, the radiance value observed at each point in the scene consists of two components: *direct* and *global* [10]. The direct component such as (direct) *specular* reflection and (direct) *diffuse* reflection is caused by the direct illumination from the light source itself. On the other hand, the global component is caused by the illumination from the other points in the scene due to inter-reflection, subsurface scattering, volumetric scattering, diffusion, and so on. Separating those components of a scene is important for various CV and CG applications such as shape recovery, image-based material editing, and improving image quality [10, 9, 4, 17].

In a *static* scene, we can separate specular and diffuse reflection components on the basis of polarization by using a rotating linear polarizer in front of a light source and a camera with a fixed linear polarizer [18] or a light source with a fixed linear polarizer and a polarization camera. This is because specular reflection components are polarized but diffuse reflection components are unpolarized. On the other hand, we can separate direct and global components by projecting spatially high-frequency patterns from a projector [10], because the global components are low-frequency in general. Therefore, those techniques can be combined for separating specular, diffuse, and global components of a static scene. Unfortunately, however, a straightforward combination of those techniques is not applicable to dynamic scenes, since the frame rates of off-the-shelf projectors and polarization cameras are not so high in general.

In this paper, we propose a method for fast separation of specular, diffuse, and global components of a *dynamic* scene by using a projector-camera system [12, 3, 2, 1]. The key idea of our proposed method is to change not only the spatial patterns but also the polarization states of illumination rapidly by using a self-build polarization projector. Our polarization projector is based on a DLP (Digital Light Processing) projector; we replace a rotating color wheel in a DLP projector with a rotating linear polarizer. Then, the image sequence of the scene is captured by using a high-speed camera so that the effects of the rapidly-varying illumination conditions on the scene are observed.

Our proposed method investigates the image sequence of a scene, when the input to our polarization projector is a single high-frequency pattern. Note that the output from the projector rapidly changes in both polarization states and intensities because of the rotating linear polarizer and the temporal dithering [9] due to DMD (Digital Mirror Device) even for a single input pattern. Our method uses a reference object, and then does not require projector-camera temporal synchronization and automatically calibrates the correspondence between the projection pattern and the camera pixel even in a dynamic scene. Furthermore, in order to improve the quality of the separated images, our method optimizes the projection pattern on the basis of noise propagation analysis, makes use of the 3D mode in the side-by-side format of a projector for rapidly shifting the projection pattern, and introduces pixel weights for taking spatial correlation into consideration.

The main contribution of this study is threefold. First, we achieve fast separation of specular, diffuse, and global components with 60 fps by exploiting the rapidly-varying polarization states and the temporal dithering of our self-build polarization projector. Second, our proposed method is easy-to-implement, because it does not require projector-camera temporal synchronization and achieves auto-calibration of the projection pattern-camera pixel correspondence. Third, our method is robust due to the optimized and shifted projection pattern and the incorporated spatial correlation.

The rest of this paper is organized as follows. In Section 2, we briefly summarize related work. In Section 3, our polarization projector is introduced, and a method for fast separation of specular, diffuse, and global components of a dynamic scene is proposed. We report the experimental results in Section 4 and present concluding remarks in Section 5.

2 Related Work

2.1 Specular-diffuse separation

In general, the reflected light observed on an object surface consists of a diffuse reflection component and a specular reflection component. Shafer [14] proposes a method for specular-diffuse separation based on the difference of their colors. Specifically, the color of a specular reflection component is the same as the color of a light source, but the color of a diffuse reflection component depends on the reflectance of a surface according to the dichromatic reflection model.

We can separate specular and diffuse reflection components on the basis of the low-rank structure of diffuse reflection components under varying light source directions. Specifically, the image of a Lambertian object under an arbitrary directional light source is represented by the linear combination of three basis images of the object [15]. The low-rank structure is used for separating specular and diffuse reflection components of the images taken under a multi-spectral light stage [6].

We can separate specular and diffuse reflection components on the basis of the difference of the polarization states of a specular reflection component and a diffuse reflection component. Specifically, when we observe the reflected light from an object surface illuminated by polarized light, the former is polarized whereas the latter is unpolarized [18]. The polarization-based approach requires a set of images taken by placing linear polarizing filters in front of a light source and a camera, and rotating one of them.

In contrast to the above existing methods, we propose a method for separating specular, diffuse, and global components of a scene by using a projector-camera system. We separate not only specular and diffuse reflection components within direct components but also global components by projecting spatially high-frequency patterns.

2.2 Direct-global separation

The direct-global separation reveals how the light radiated from a light source interacts with a scene. Nayar *et al.* [10] propose a method for separating direct and global components in a scene by projecting high-frequency patterns from a projector on the basis of the insight that global components are spatially low-frequency in general.

Gu *et al.* [4] extend the above direct-global separation for a single light source to that for multiple light sources. Specifically, they optimize a set of high-frequency projection patterns in terms of SNR (signal-to-noise ratio) on the basis of illumination multiplexing [13], and then show that it is effective for scene recovery. Mukaigawa *et al.* [8] show that projecting high-frequency patterns is useful also for studying the light transport in scattering media, in particular for decomposing multiple scattering into each bounce component.

In contrast to the above existing methods, we propose a method for separating specular, diffuse, and global components of a scene. In other words, we further separate the direct components into specular and diffuse reflection components on the basis of polarization.

2.3 Active illumination using DLP projector

Narasimhan *et al.* [9] propose a method for separating direct and global components of a dynamic scene by using a DLP projector and a high-speed camera on the basis of the temporal dithering, *i.e.* the rapid changes in intensities due to the DMD in a DLP projector. They show that the temporal dithering is useful also for fast active vision such as structured light-based range finding and photometric stereo.

On the other hand, Han *et al.* [5] propose a method for recovering the spectral reflectance of a moving object by using a DLP projector and a high-speed camera on the basis of the color switch, *i.e.* the rapid changes in colors due to the rotating color wheel in a DLP projector. Maeda and Okabe [7] exploit the rapidly-varying illumination colors due to the color switch of a multi-primary DLP projector, and then propose a method for separating direct and global components of a static scene per primary color of the projector by using an usual camera with a short exposure time. In addition, they propose a method for estimating the SPDs (Spectral Power Distributions) of the primary colors in a non-destructive manner.

Torii *et al.* [17] exploit both the color switch and the temporal dithering of a DLP projector, and achieve the direct-global separation of dynamic scenes per illumination color. Their method is not a straightforward combination of the above existing methods based on the temporal dithering [9] and the color switch [7]. In particular, they realize auto-calibration of the projection pattern-camera pixel correspondence on the basis of the consistency in pixel intensities. Furthermore, they optimize the high-frequency projection pattern on the basis of noise propagation analysis so that it is robust to noises.

In contrast to the above existing methods, in particular to Torii *et al.* [17], we exploit polarization. Specifically, by replacing a rotating color wheel with a rotating linear polarizer, we exploit the rapid changes in not colors but polarization states for fast separation of specular, diffuse, and global components.

3 Proposed Method

3.1 Principle of direct-global separation

Nayar *et al.* [10] propose a method for direct-global separation of a static scene by using a projector-camera system. It exploits the properties of global components, *i.e.* they are spatially low-frequency in general, and studies the images of the scene under high-frequency projection patterns. Specifically, their simplest method uses two images; they are captured when a black-and-white checkered pattern or its negative-positive reversed pattern are projected from a projector to the scene.

Let us denote the two output intensities from a projector corresponding to white and black input intensities of a checkered pattern by a and b, *e.g.* $a = 1$ and $b = 0$. The pixel values observed at a certain point in a scene are given by

$$I^+ = aL_D + \frac{1}{2}(a+b)L_G, \tag{1}$$

$$I^- = bL_D + \frac{1}{2}(a+b)L_G, \tag{2}$$

where L_D and L_G are the direct and global components at the point, and I^+ and I^- are the larger and smaller pixel values observed there, when $a > b$ [10, 9]. Therefore, we can obtain the direct component L_D and the global component L_G by solving the simultaneous linear equations in eq.(1) and eq.(2), when the pixel values I^+ and I^- and the output intensities from the projector a and b are given.

3.2 Principle of specular-diffuse separation

Wolff and Boult [18] show that specular and diffuse reflection components can be separated on the basis of polarization, since specular reflection components are polarized but diffuse reflection components are unpolarized. Specifically, they propose a method for specular-diffuse separation of a static scene by using a rotating linear polarizer in front of a light source and a camera with a fixed linear polarizer or a light source with a fixed linear polarizer and a rotating linear polarizer in front of a camera. Recently, we can replace the pair of the camera and the rotating linear polarizer with a single polarization camera in the latter setup.

Let us consider the latter case, *i.e.* a light source with a fixed linear polarizer and a rotating linear polarizer in front of a camera. The pixel values observed at a certain point in a scene are given by

$$I_{\max} = L_s + \frac{1}{2}L_d, \tag{3}$$

$$I_{\min} = \frac{1}{2}L_d, \tag{4}$$

where L_s and L_d are the specular and diffuse reflection components at the point, and $I_{\max}$ and $I_{\min}$ are the maximal and minimal pixel values observed there, when the linear polarizer is rotated in front of the camera. Therefore, we can obtain the specular reflection component L_s and the diffuse reflection component L_d by solving the simultaneous linear equations in eq.(3) and eq.(4), when the pixel values $I_{\max}$ and $I_{\min}$ are given.

3.3 Self-build polarization projector

Both the methods for direct-global separation and specular-diffuse separation require multiple images taken under different spatial patterns and with different polarization states. Note that we still require multiple images taken under

Fig. 1. Our self-build polarization projector based on a DLP projector. The rotating color wheel in the DLP projector is replaced with a rotating linear polarizer.

different spatial patterns, even if we use a polarization camera. Therefore, a straightforward combination of those techniques is not applicable to dynamic scenes, since the frame rates of off-the-shelf projectors and polarization cameras are not so high in general[4].

Accordingly, our proposed method rapidly changes not only the spatial patterns but also the polarization states of illumination by using a self-build polarization projector. Our polarization projector is based on a DLP projector. In a single-chip DLP projector, a color wheel consisting of three (or more) color filters with different spectral transmittances is placed between a white lamp and a DMD. The color wheel rotates at high speed in front of the lamp, and generates various colors by mixing the transmitted lights with different SPDs via time-division multiplexing. Then, the DMD controls the intensity of the light transmitted from the color wheel by temporal dithering; it switches micro mirrors "on" and "off" directions at high speed. We replace the rotating color wheel in a DLP projector with a rotating linear polarizer as shown in Fig. 1; the linear polarizer is installed outside the projector housing in order to prevent heat damage due to the projector lamp.

3.4 Specular-diffuse-global separation

Fig. 2(a) shows our setup for separating specular, diffuse, and global components by using a projector-camera system. Specifically, a scene of interest is illuminated by our polarization projector, and its images are captured by using a high-speed camera through a fixed linear polarizer. The input to the projector is a single checkered pattern with two intensities, but the output from the projector rapidly changes in both the polarization states and intensities due to the rotating linear polarizer and DMD respectively.

The propagation of the polarized light is computed by using the Stokes vectors and Mueller matrices. We can derive that the pixel value I_n observed at a certain point in a scene at the n-th frame $(n = 1, 2, 3, ..., N)$ is given by

$$I_n = a_n L_s[\cos 2(\chi_n + \phi) + 1] + a_n L_d + \frac{1}{2}(a_n + b_n)L_G \tag{5}$$

[4] See the experimental results and discussion in Section 4.3 for more detail.

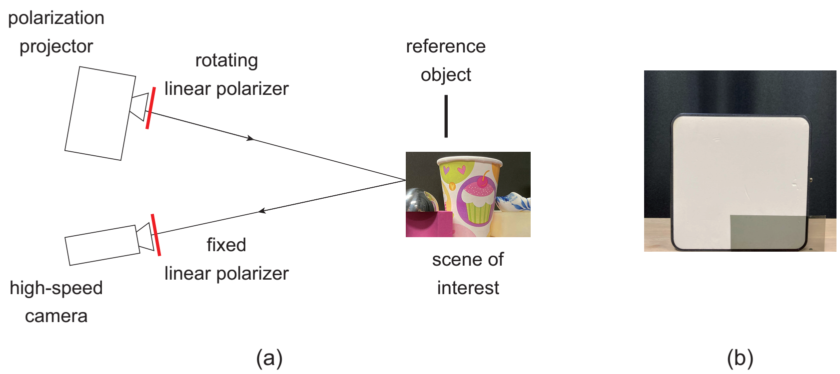

Fig. 2. (a) Our setup for separating specular, diffuse, and global components. A scene of interest is illuminated by our polarization projector, and its images are captured by using a high-speed camera through a linear polarizer. (b) Our reference object; a part of a white diffuse target is covered by a linear polarizer.

or

$$I_n = b_n L_s[\cos 2(\chi_n + \phi) + 1] + b_n L_d + \frac{1}{2}(a_n + b_n) L_G, \tag{6}$$

when the point is directly illuminated by the checkered pattern with the output intensity of a_n or b_n. Here, L_s, L_d, and L_G are the specular, diffuse, and global components to be estimated, a_n and b_n are the output intensities from the projector, and χ_n and ϕ are the polarization angle of the projected light and the pixel-wise phase of the polarization angle respectively.

Our proposed method assumes that the scene is approximately static while N images are captured by using a high-speed camera, *e.g.* 16 msec in our experiments, and that the output intensities a_n and b_n and the polarization angle χ_n of the projected light are known (see Section 3.5 for more detail). Then, our method estimates the specular, diffuse, and global components and the phase of the polarization angle from N images by solving the set of equations in eq.(5) or eq.(6). Specifically, we fix the phase ϕ of the polarization angle to a certain value, and then solve the simultaneous linear equations in eq.(5) or eq.(6) with respect to L_s, L_d, and L_G by least squares. We change the value of the phase in a coarse-to-fine manner, and find the optimal L_s, L_d, L_G, and ϕ with the minimal least-square errors.

3.5 Auto spatio-temporal calibration

Our proposed method calibrates the output intensities a_n and b_n and the polarization angle χ_n by using a reference object placed in a scene of interest and captured at the same time. It consists of a white diffuse target and a linear polarizer; a part of the white diffuse target is covered by the linear polarizer as shown in Fig. 2(b). Specifically, we calibrate the output intensities a_n and b_n from the pixel values of the white target object and compute the polarization angle χ_n from the pixel values when the white target object is illuminated and observed through the linear polarizer. Thus, our method calibrates a_n, b_n, and χ_n from the captured images in situ, and therefore it does not require projector-camera temporal synchronization.

In order to solve the set of equations in eq.(5) or eq.(6), we need to calibrate the correspondence between the projection pattern and the camera pixel. In other words, we need to known which block, whose output intensity is a_n or b_n, directly illuminates each point in a scene. To this end, we select two images whose polarization angles are almost the same $\chi_n \simeq \chi_m$ and output intensities satisfy $a_n > a_m$, $b_n < b_m$, and $(a_n + b_n) \simeq (a_m + b_m)$, and study the difference between I_n and I_m. Because $(I_n - I_m)$ is proportional to $(a_n - a_m)$ or $(b_n - b_m)$ according to the correspondence between the projection pattern and the camera pixel, we can calibrate the correspondence from the sign of $(I_n - I_m)$.

3.6 Optimizing projection pattern

The output intensities from our DLP-based polarization projector, *i.e.* how the output intensities vary due to the temporal dithering depends on the input intensities to the projector. Therefore, we can optimize the two input intensities of the checkered pattern in order to separate specular, diffuse, and global components robustly. We take account of the noises in the observed pixel values, and then optimize those input intensities on the basis of the noise propagation analysis.

Specifically, we study the sum of the condition numbers [11] of the coefficient matrices of the set of equations in eq.(5):

$$\begin{pmatrix} a_1[\cos 2(\chi_1 + \phi) + 1] & a_1 & (a_1 + b_1)/2 \\ a_2[\cos 2(\chi_2 + \phi) + 1] & a_2 & (a_2 + b_2)/2 \\ \vdots & \vdots & \vdots \\ a_N[\cos 2(\chi_N + \phi) + 1] & a_N & (a_N + b_N)/2 \end{pmatrix}, \tag{7}$$

and in eq.(6):

$$\begin{pmatrix} b_1[\cos 2(\chi_1 + \phi) + 1] & b_1 & (a_1 + b_1)/2 \\ b_2[\cos 2(\chi_2 + \phi) + 1] & b_2 & (a_2 + b_2)/2 \\ \vdots & \vdots & \vdots \\ b_N[\cos 2(\chi_N + \phi) + 1] & b_N & (a_N + b_N)/2 \end{pmatrix}, \tag{8}$$

where N is the number of the captured images from which we compute the specular, diffuse, and global components of a single frame. The condition number tells how much noises in the observation I_n propagate to the unknowns to be estimated; L_s, L_d, and L_G[5]. We compute the condition numbers for all the pairs

[5] We assume $\phi = 0$ when computing the condition numbers. We tested other values, but the condition numbers were almost constant with respect to ϕ.

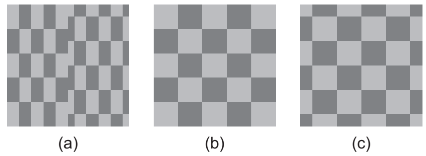

Fig. 3. The 3D mode in the side-by-side format: (a) a single input image, (b) an output image for left eye, and (c) an output image for right eye.

of the input intensities in 8 bit (from 0 to 255), and then select the optimal pair of the input intensities from 32,640 ($= {}_{256}C_2$) pairs. Note that smaller condition number is better.

3.7 Use of 3D mode in side-by-side format

The simplest direct-global separation described in Section 3.1 uses two projection patterns; one is a black-and-white checkered pattern and the other is its negative-positive reversed pattern. It is known that the simplest method often causes visible artifacts near the boundaries between the blocks of the checkered pattens, because the spatial resolutions of a projector and a camera are limited. Nayar *et al.* [10] show that those artifacts can be reduced by using more than two projection patterns, e.g. spatially shifted patterns from the original checkered patten.

Accordingly, our proposed method makes use of the 3D mode in the side-by-side format, which is relatively common function even for consumer projectors, and then projects two spatially-shifted checkered patterns. When a single image in Fig. 3 (a) is input to the projector, the projector outputs (b) a left-eye image and (c) a right-eye image in turn. Since we can distinguish the two spatially-shifted checkered patterns from the pixel values on the reference object, we can realize the specular, diffuse, and global separation by using spatially-shifted projection patterns in a similar manner to the case without the 3D mode.

3.8 Incorporating spatial correlation

In addition to the optimized and quickly-shifted projection pattern in Section 3.6 and Section 3.7, we further improve the quality of the separated images by taking the spatial correlation into consideration. Specifically, our proposed method solves the set of equations in eq.(5) or eq.(6) from not only the pixel values observed at a certain point pixel-wisely but also those at surrounding pixels by weighted least squares.

We introduce a single weight per pixel, *i.e.* per set of equations in eq.(5) or eq.(6). The weight is given by the product of three Gaussian weights. The first one depends on the distance between the pixels, and the second one depends on the difference between the pixel values when the output intensities are almost

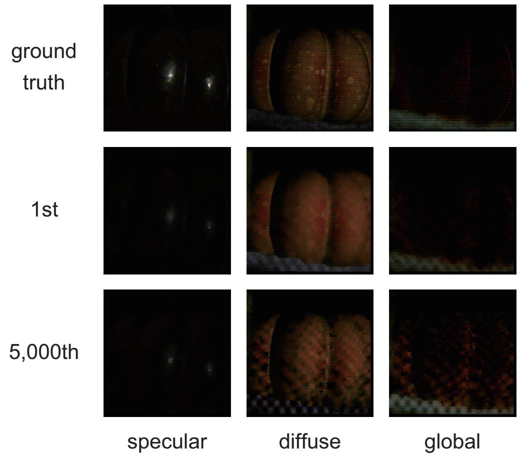

Fig. 4. The ground truth images (top row), our result images using the best (middle row) and the 5,000th best (bottom row) combinations of the input intensities of the checkered pattern.

Table 1. The quantitative comparison of Fig. 4. The numerical values in each cell are the PSNR (upper) and SSIM (lower).

	specular	diffuse	global	average
ours:	**30.29**	26.38	**32.85**	**29.84**
1st	0.733	**0.797**	**0.774**	**0.768**
ours:	30.18	**27.41**	26.82	28.14
5,000th	**0.749**	0.776	0.608	0.711

the same, *i.e.* $a_n \simeq b_m$. Therefore, the product of those weights is similar to the weight for the bilateral filter [16]. The third weight has small/large values if the pixel is close to/far from the boundaries between the blocks of the checkered patten. The boundaries are detected from the zero crossing of the difference $(I_n - I_m)$ (see Section 3.5 for more detail).

4 Experiments

4.1 Experimental setup

In our experiments, we used a self-build polarization projector based on a DLP projector MH534 from BenQ and a high-speed camera Fastcam Mini UX50 from Photron. The 3D mode of the projector quickly switches the left-eye and right-eye images in about 8 msec (about 120 fps), and one revolution of the rotating linear

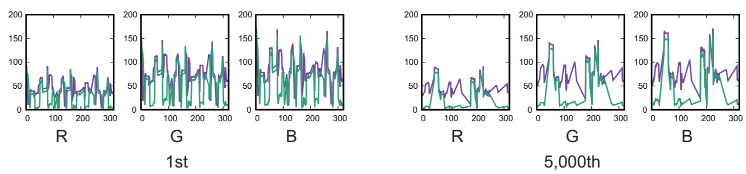

Fig. 5. The output intensities a_n and b_n of each color channel for the 1st and the 5,000th best combinations.

polarizer takes about 14 msec[6]. The frame rate and the exposure time of the high-speed camera were set to 10,000 fps and 0.1 ms respectively. Therefore, our proposed method achieves specular, diffuse, and global separation from about 160 images in about 60 fps. As described in Section 3.5, we optimized the pixel intensities of the input checkered pattern, and then set them to 255 and 203 for the left-eye image and 255 and 210 for the right-eye image.

4.2 Experimental results for static scenes

We tested our proposed method on static scenes for quantitative evaluation. In a static scene, we can acquire the ground truth images of specular, diffuse, and global components by using a number of spatially high-frequency patterns. Specifically, we used 50 ($= 2 \times 5 \times 5$) projection patterns; a black-and-white checkered pattern and its reversed pattern were sifted along the horizontal and vertical directions 5 times respectively.

Optimization of projection pattern: First, we confirm the effectiveness of the optimized projection pattern. Fig. 4 shows the ground truth images (top row), our result images using the best (middle row) and the 5,000th best (bottom row) combinations of the input intensities of the checkered pattern. This scene consists of a plastic pumpkin with specular and diffuse components and cotton with global components. The pixel intensities of the 5,000th best combinations are 169 and 45 for the left-eye image and 215 and 156 for the right-eye image.

We can see that our method using the best combination works better than that using the 5,000th best combination; block artifacts are more visible in the result images using the 5,000th best combination. The PSNR and SSIM of the result images in Table 1 quantitatively show the effectiveness of the optimized projection pattern.

Note that the separation using the 5,000th best combination was not robust; we sometimes could not solve the set of equations in eq.(5) or eq.(6) due to ill-

[6] The revolving speed is slower than the original color wheel, because our linear polarizer has larger moment.

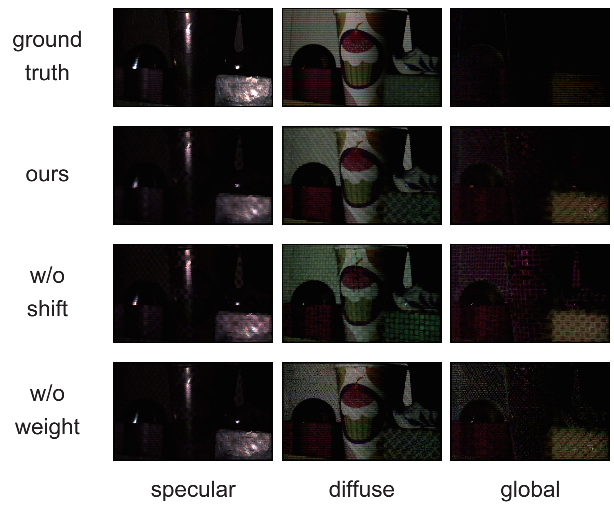

Fig. 6. The ground truth images (top row), our result images (second row) , those without shift (third row) and weight (fourth row).

Table 2. The quantitative comparison of Fig. 6. The numerical values in each cell are the PSNR (upper) and SSIM (lower).

	specular	diffuse	global	average
ours	22.44	**24.60**	**25.01**	**24.02**
	0.720	**0.703**	**0.498**	**0.640**
w/o	**22.98**	22.61	21.78	22.46
shift	0.718	0.610	0.358	0.562
w/o	22.81	23.02	22.81	22.88
weight	**0.740**	0.688	0.405	0.611

conditioned problems, and then some of the result images are collapsed. Fig. 5 shows the output intensities a_n and b_n of each color channel for the 1st and the 5,000th best combinations. We can see that the output intensities of the 1st combinations significantly vary and would yield better condition numbers for solving eq.(5) or eq.(6).

3D mode for shifting projection pattern: Second, we confirm the effectiveness of the 3D mode for quickly shifting projection pattern. Fig. 6 shows the ground truth images (top row), our result images with (second row) and without (third row) shift. This scene includes a mirror hemisphere with specular components, a paper cup with specular and diffuse components, a ceramic shoe with specular and diffuse components, and a soap with global components.

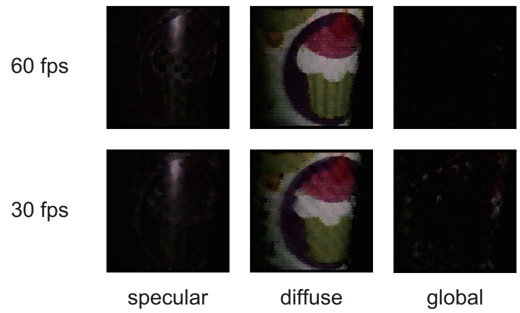

Fig. 7. Our result images with 60 fps (upper) and 30 fps (lower).

We can see that line artifacts corresponding to the boundaries between the blocks of the checkered pattern are more visible in the result images without shift. Comparing the PSNR and SSIM of those results in Table 2, the effectiveness of the 3D mode for shifting projection pattern is clear quantitatively.

Weights for incorporating spatial correlation: Third, we confirm the effectiveness of the weights for incorporating spatial correlation. Fig. 6 shows the ground truth images (top row), our result images with (second row) and without (fourth row) the weights for incorporating spatial correlation. We empirically set the standard deviations of the Gaussian weights in Section 3.8.

We can see that the result images taking spatial correlation into consideration are smoother than those without spatial correlation, *i.e.* pixel-wise separation. Table 2 quantitatively shows the effectiveness of incorporating spatial correlation into specular, diffuse, and global separation.

4.3 Experimental results for dynamic scenes

Our proposed method achieves fast separation of specular, diffuse, and global components with about 60 fps. Since we capture the effects of the temporal dithering by using a high-speed camera, our method requires only a single projection pattern, *i.e. two* projection patterns in fact: a checkered pattern with gray intensities for the left-eye image and a shifted checkered pattern with gray intensities for the right-eye image.

On the other hand, consumer polarization cameras cannot capture the effects of the temporal dithering, because their frame rates are not so high. Then, separating specular, diffuse, and global components by using a pair of a polarized light source and a polarization camera requires projector-camera temporal synchronization and *four* projection patterns; a black-and-white checkered pattern, its negative-positive reversed pattern, and their shifted patterns. Therefore, the frame rate of the polarization camera-based method is half in theory, if a projector has the same frame rate as ours.

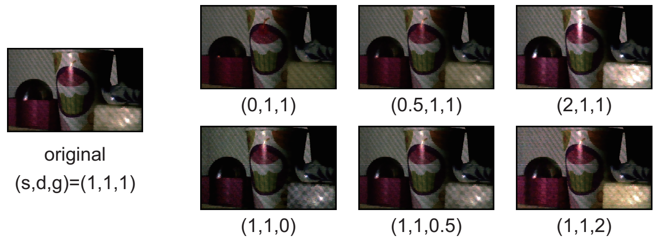

Fig. 8. Application to image-based material editing. The glossiness (upper) and translucency (lower) are edited.

Accordingly, we compared the performance of our proposed method for varying temporal resolution. Fig. 7 shows the result images with 60 fps and 30 fps. The latter corresponds to the frame rate of the polarization camera-based method. The object is a paper cup in motion. We can see that the texture on the paper cup is blurred due to motion in the result images with 30 fps. This result demonstrates the advantage of our method over the polarization camera-based method.

4.4 Application to image-based material editing

As a direct application of our specular, diffuse, and global separation, we conducted image-based material editing. Specifically, we synthesized various image sequences by linearly combining the separated components with different weights; s, d, and g for the specular, diffuse, and global components. Fig. 8 shows the original and synthesized images of a single frame; the glossiness and translucency are edited in the images at the upper and lower rows respectively. We can see that our proposed method is effective for photorealistic image-based material editing.

5 Conclusion and Future Work

We proposed a fast, robust, and easy-to-implement method for separating specular, diffuse, and global components of a dynamic scene by using a projector-camera system. Specifically, our proposed method exploits the rapidly-varying illumination conditions due to both the rotating linear polarizer and the temporal dithering. We conducted a number of experiments using our prototype setup and showed the effectiveness of our method and its components: the optimization of projection pattern, the use of the 3D mode for quickly shifting projection pattern, and the weights for incorporating spatial correlation. Our future study includes the extension to colored and polarized pattern projection; we can integrate a color wheel and a linear polarizer into a single colored and polarized filter for multispectral and polarimetric scene analysis.

Acknowledgments

This work was supported by JSPS KAKENHI Grant Numbers JP20H00612 and JP17H01766.

References

1. Amano, T.: Shading illusion: a novel way for 3-D representation on the paper media. In: Proc. PROCAMS2012 (2012)
2. Bimber, O., Iwai, D., Wetzstein, G., Grundhöfer, A.: The visual computing of projector-camera systems. Computer Graphics Forum **27**(8), 2219–2245 (2008)
3. Grossberg, M., Peri, H., Nayar, S., Belhumeur, P.: Making one object look like another: controlling appearance using a projector-camera system. In: Proc. IEEE CVPR2004. pp. I–452–459 (2004)
4. Gu, J., Kobayashi, T., Gupta, M., Nayar, S.: Multiplexed illumination for scene recovery in the presence of global illumination. In: Proc. IEEE ICCV2011. pp. 691–698 (2011)
5. Han, S., Sato, I., Okabe, T., Sato, Y.: Fast spectral reflectance recovery using DLP projector. IJCV **110**(2), 172–184 (2014)
6. Kobayashi, N., Okabe, T.: Separating reflection components in images under multispectral and multidirectional light sources. In: In Proc. ICPR2016. pp. 3199–3204 (2016)
7. Maeda, K., Okabe, T.: Acquiring multispectral light transport using multi-primary DLP projector. In: Proc. IPTA2016. pp. 1–6 (2016)
8. Mukaigawa, Y., Yagi, Y., Raskar, R.: Analysis of light transport in scattering media. In: Proc. IEEE CVPR2010. pp. 153–160 (2010)
9. Narasimhan, S., Koppal, S., Yamazaki, S.: Temporal dithering of illumination for fast active vision. In: Proc. ECCV2008. pp. 830–844 (2008)
10. Nayar, S., Krishnan, G., Grossberg, M., Raskar, R.: Fast separation of direct and global components of a scene using high frequency illumination. In: Proc. ACM SIGGRAPH 2006. pp. 935–944 (2006)
11. Press, W., Teukolsky, S., Vetterling, W., Flannery, B.: Numerical Recipes in C 3rd Edition: The Art of Scientific Computing. Cambridge University Press (2007)
12. Raskar, R., Welch, G., Low, K.L., Bandyopadhyay, D.: Shader lamps: animating real objects with image-based illumination. In: Proc. EWRT2001. pp. 89–102 (2001)
13. Schechner, Y., Nayar, S., Belhumeur, P.: A theory of multiplexed illumination. In: Proc. IEEE ICCV2003. pp. 808–815 (2003)
14. Shafer, S.: Using color to separate reflection components. Color Research & Application **10**(4), 210–218 (1985)
15. Shashua, A.: On photometric issues in 3D visual recognition from a single 2D image. IJCV **21**(1/2), 99–122 (1997)
16. Tomasi, C., Manduchi, R.: Bilateral filtering for gray and color images pp. 839–846 (1998)
17. Torii, M., Okabe, T., Amano, T.: Multispectral direct-global separation of dynamic scenes. In: Proc. IEEE WACV2019. pp. 1923–1931 (2019)
18. Wolff, L., Boult, T.: Constraining object features using a polarization reflectance model. IEEE Trans. PAMI **13**(6), 167–189 (1991)